

# Influence of randomly distributed magnetic nanoparticles on surface superconductivity in Nb films

D. Stamopoulos, M. Pissas, V. Karanasos, and D. Niarchos

*Institute of Materials Science, NCSR "Demokritos," 153-10, Aghia Paraskevi, Athens, Greece*

I. Panagiotopoulos

*Department of Materials Science and Engineering, University of Ioannina, Ioannina 45110, Greece*

(Received 25 June 2003; revised manuscript received 29 March 2004; published 19 August 2004)

We report on combined resistance and magnetic measurements in a hybrid structure (HS) of randomly distributed anisotropic CoPt magnetic nanoparticles (MN) embedded in a 160 nm Nb thick film. Our resistance measurements exhibited a sharp increase at the magnetically determined bulk upper-critical fields  $H_{c2}(T)$ . Above these points the resistance curves are rounded, attaining the normal state value at much higher fields identified as the surface superconductivity fields  $H_{c3}(T)$ . When plotted in reduced temperature units, the characteristic field lines  $H_{c3}(T)$  of the HS and of a pure Nb film, prepared at exactly the same conditions, coincide for  $H < 10$  kOe, while for fields  $H > 10$  kOe they strongly segregate. Interestingly, the characteristic value  $H = 10$  kOe is equal to the saturation field  $H_{\text{sat}}^{\text{MN}}$  of the MN. The behavior mentioned above is observed only for the case where the field is normal to the film's surface, while it is absent when the field is parallel to the film. Our experimental results suggest that the observed enhancement of surface superconductivity field  $H_{c3}(T)$  is possibly due to the not uniform local reduction of the external magnetic field by the dipolar fields of the MN.

DOI: 10.1103/PhysRevB.70.054512

PACS number(s): 74.25.Op, 74.78.Db, 74.25.Fy, 74.25.Dw

## I. INTRODUCTION

The interplay of superconductivity with magnetism is an interesting subject of current theoretical and experimental research. The interest on the experimental study of composite superconductor–ferromagnet (SC/FM) structures is continuous not only due to their importance for the further theoretical treatment and understanding of the underlying mechanisms, but also because of the promising applications that such combined structures could give in the near future.<sup>1,2</sup> Such composite structures are in the form of films consisting of SC/FM bilayers or superlattices,<sup>2–4</sup> periodic nanosized or microsized artificial FM dots or squares embedded in a low- $T_c$  superconducting film,<sup>5–13</sup> etc.

In such artificial structures there are two basic mechanisms that control the interaction between the superconducting order parameter and the magnetic moments at the SC/FM interface. First is the electromagnetic mechanism which is related to the interaction of the superconducting pairs with the magnetic fields induced by the FM component in the SC and second is the exchange interaction that the superconducting pairs experience as they enter the FM through the SC/FM interface.<sup>14–16</sup> This second mechanism plays a crucial role when the SC and the FM layers are placed in close proximity and the SC/FM interfaces are of high structural quality. In such cases the so-called proximity effect dominates and a number of interesting phenomena are revealed. In the proximity effect the spin dependence of the exchange interaction in the FM results in a favorable spin orientation for the superconducting electrons. As a consequence the superconducting pairs are destroyed as they are transmitted through the SC/FM interface. Nevertheless, in many cases the superconducting pairs may be reflected, rather than transmitted, at the

SC/FM interface. A phenomenological parameter called transparency is employed to describe the transmission ability of the interface.<sup>17,18</sup> This parameter depends on the structural quality of the interface and on the specific spin-dependent scattering mechanism that the superconducting pairs experience.<sup>17–22</sup> In the case of very low transparency the superconducting pairs never enter the FM as they are reflected at the SC/FM interface. As a consequence the proximity effect is depressed. In contrast, when nearly perfect interfaces are available their transparency is very high and consequently the proximity effect is fully restored with breaking of the transmitted pairs to occur in the FM. Nevertheless, the whole process is not instant but occurs at a time scale corresponding to a travelling length of the order of the coherence length  $\xi_F$  in the FM. Even in the clean limit where  $\xi_F = \hbar u_F / \Delta E_{\text{ex}}$  ( $u_F$  is the Fermi velocity and  $\Delta E_{\text{ex}}$  is the exchange splitting) the characteristic magnetic length is very small and as a result the superconducting order parameter exhibits a rapid decay in the FM component. As a consequence of its almost zeroing at the SC/FM interface the superconducting order parameter should also be strongly depressed at a scale of the order of the coherence length  $\xi_S$  in the SC.<sup>23,24</sup> Thus, it is generally expected that at a SC/FM interface the proximity effect should be antagonistic to the nucleation of superconductivity near the surfaces of the SC.

On the other hand, when a SC is in proximity with an insulator (IN) superconductivity should firstly appear not in the bulk of the SC but at a thin layer of the order of  $\xi_S$  near its surfaces.<sup>25</sup> This is the so-called surface superconductivity effect and occurs at a magnetic field  $H_{c3}(T)$  which is higher than the bulk upper-critical field  $H_{c2}(T)$  where superconducting order is established in the whole sample.<sup>25,26</sup> As a consequence of the surface superconducting layer for

$H < H_{c3}(T)$  the magnetoresistance is lower than the normal state value and becomes zero only when bulk superconductivity occurs, i.e., at  $H = H_{c2}(T) < H_{c3}(T)$ . In contrast, it is expected that in the regime  $H_{c2}(T) < H < H_{c3}(T)$  the measured magnetization of the superconductor should be zero due to a change in the direction of the superconducting screening currents that flow in the thin layer near the surface of the sample.<sup>25,26</sup> Thus, the effect of surface superconductivity cannot be identified by means of global magnetic measurements (SQUID measurements).

Until today, most of the reports on HS referred mainly to transport properties performed in the regime just below the bulk upper-critical field  $H_{c2}(T)$ , or well inside the mixed state of the superconductor and were limited in the low-field regime close to the critical temperature. The influence of a magnetic component to the transport behavior of the superconductor in the high-field regime above the bulk upper-critical field  $H_{c2}(T)$  and especially the behavior of the surface superconductivity field  $H_{c3}(T)$  has not attracted the interest of experimental studies although there are theoretical reports related to the subject.<sup>14,15,27</sup> In this paper we present detailed transport and magnetic data on the influence of randomly distributed anisotropic CoPt MN on the superconducting order parameter of the conventional low- $T_c$  Nb superconductor which is a simple isotropic system, thus giving us the opportunity to exclude parameters (thermal fluctuations or anisotropy) that could complicate the total behavior of a HS. In the composite system, we found that the surface superconductivity field  $H_{c3}(T)$  is strongly enhanced in the high-field regime when the applied field is normal to the film's surface. More specifically, we found that although the related lines  $H_{c3}(T)$  of the HS and pure Nb films coincide in the low-field regime  $H < 10$  kOe, they strongly segregate for  $H > 10$  kOe. The characteristic value  $H = 10$  kOe where this change occurs is equal to the saturation field  $H_{\text{sat}}^{\text{MN}}$  of the MN. In contrast, the bulk upper-critical lines  $H_{c2}(T)$  of the pure Nb and the HS films almost coincide. A comparison of our experimental results with current theoretical knowledge is made and a simple explanation is proposed for the observed behavior. We believe that in our case the electromagnetic mechanism plays a dominant role, while the proximity effect is probably depressed due to the low transparency of the structurally disordered surfaces of the MN. The high values that the dipolar field of the MN attains by their lateral surfaces results in a sufficient reduction of the external applied magnetic field in the respective regimes. As a result the surface superconductivity field line  $H_{c3}(T)$  is strongly enhanced in the HS film.

## II. PREPARATION OF THE FILMS AND EXPERIMENTAL DETAILS

First of all, our aim was to produce pure Nb films. Relatively clean films are needed in order to minimize the bulk pinning of vortices. This is necessary in order to reveal the interaction between the MN and the superconducting order parameter. The sputtering conditions needed for the deposition of relatively clean Nb films and for the preparation of the CoPt MN are reported in Refs. 28 and 29, respectively.

The CoPt MN are isolated and randomly distributed on the substrate's surface. Their magnetic behavior is anisotropic, presenting a preferential out-of-plane magnetic moment. Their typical in-plane size and thickness are of the order of 200 nm and 30 nm, respectively, while their distance is of the order of 200 nm (see transmission electron microscopy data in Ref. 29). After producing the MN the Nb layer was sputtered on top of them, so that the MN were actually embedded at the bottom of the Nb layer (see Fig. 7 below). We should underline that the pure Nb film and the Nb layer of the HS were produced simultaneously during the same sputtering run since the two substrates were mounted side by side. In this way the same intrinsic properties of the Nb layer of the HS and of the pure Nb film are obtained. The critical temperature of the films under discussion is  $T_c = 8.3$  K for pure Nb and  $T_c = 7.7$  K for the HS. The residual resistance ratio is  $\text{RRR} \approx 3$ . The determination of the thickness of the Nb layer was based on an Alpha-Step device and for the films under discussion was found to be  $\approx 160$  nm ensuring that the SC is in the three-dimensional (3D) bulk limit. Typical in plane dimensions of the films are  $4 \times 4$  mm<sup>2</sup>. Combined x-ray diffraction and transmission electron microscopy data revealed that the crystallites of the Nb layer have mean size of the order of 40 nm and that they are homogeneous without exhibiting columnar growth.

Our magnetoresistance measurements were performed by applying a dc transport current (normal to the magnetic field) and measuring the voltage in the standard four-point configuration. In most of the measurements presented below the applied current was  $I_{\text{dc}} = 0.5$  mA, which corresponds to an effective density  $J_{\text{dc}} \approx 80$  A/cm<sup>2</sup>. The magnetic measurements were performed under both zero field cooling and field cooling conditions. The temperature control and the application of the dc fields were achieved in a commercial SQUID device (Quantum Design). We examined the whole temperature-magnetic-field regime accessible by our SQUID ( $H_{\text{dc}} < 55$  kOe,  $T > 1.8$  K).

## III. EXPERIMENTAL RESULTS AND DISCUSSION

Figure 1 presents a set of magnetic and resistance measurements for magnetic fields  $H_{\text{dc}} = 5, 10,$  and  $15$  kOe normal to the surface of the HS film, while in the inset we present the magnetic data in an extended temperature regime. In the magnetic data we present both curves for zero field cooling and subsequent field cooling. We observe that the bulk upper-critical temperatures  $T_{c2}(H)$ , defined from the magnetic measurements as the point where the diamagnetic signal becomes zero, coincide with the temperatures where for a high applied current  $I_{\text{dc}} = 0.5$  mA ( $J_{\text{dc}} \approx 80$  A/cm<sup>2</sup>) the voltage starts taking nonzero values (see dotted double arrows). In addition, the magnetically determined irreversibility points  $T_{\text{irr}}(H)$  are clearly placed at much lower temperatures comparing to  $T_{c2}(H)$ . This fact indicates that the identified upper-critical points  $T_{c2}(H)$  refer to the zeroing of the equilibrium magnetization and not to a collapse of screening currents that originate from bulk pinning. More importantly, we clearly observe that the voltage curves take the normal state value at temperatures much higher than  $T_{c2}(H)$ . Furthermore,

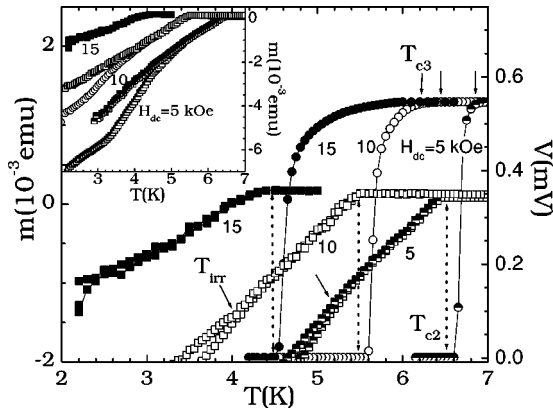


FIG. 1. The main panel presents the comparison of the measured voltage curves at a high current  $I_{dc}=0.5$  mA ( $J_{dc} \approx 80$  A/cm<sup>2</sup>) to magnetic data (circles and squares, respectively) for the HS as a function of temperature for magnetic fields  $H_{dc}=5, 10,$  and  $15$  kOe. The voltage attains the normal state value at a much higher temperature  $T_{c3}$  than the upper-critical one  $T_{c2}$ . The irreversibility points  $T_{irr}$  (inclined arrows) are clearly distinct from the bulk upper-critical temperatures  $T_{c2}$ . In the inset we present the magnetic measurements in an extended temperature regime. In all cases the applied dc field is normal to the surface of the film.

the  $I$ - $V$  characteristics exhibited a clear nonlinear behavior in the regime above  $T_{c2}(H)$  (see below). According to currently available knowledge the only characteristic effect placed outside the mixed state of a type-II superconductor [ $T > T_{c2}(H)$ ] is surface superconductivity. Thus, we identify the points where the resistance attains the normal state value as the characteristic temperatures  $T_{c3}(H)$  where surface superconductivity occurs.

In Figs. 2(a) and 2(b) we present a complete set of magnetoresistance measurements in the HS film at a constant current  $I_{dc}=0.5$  mA ( $J_{dc} \approx 80$  A/cm<sup>2</sup>) for various magnetic field values. We observe that the voltage curves are strongly rounded. The observed rounding gradually disappears as we apply lower magnetic fields. In addition, we see that the points  $T_{c3}(H)$  where the voltage takes the normal state value are well resolved in our measurements [see Fig. 2(b)] and consequently may be defined with high accuracy. In order to investigate the regime  $T_{c2}(H) < T < T_{c3}(H)$  in more detail we also performed measurements as a function of the applied current. Representative  $I$ - $V$  characteristics are shown in Fig. 3 for various temperatures at a magnetic field  $H_{dc}=20$  kOe. In the upper panel the dotted lines indicate the specific temperatures where the measurements have been performed, while the lower panel presents the respective data. For  $T < T_{c2}(H)=3.4$  K the maximum applied current  $I_{dc}=1$  mA ( $J_{dc} \approx 160$  A/cm<sup>2</sup>) does not exceed the bulk critical current and the detected voltage is almost zero. Above  $T_{c2}(H)=3.4$  K the applied current exceeds the surface critical current and a finite voltage is measured. The observed  $I$ - $V$  curves are nonlinear in the regime  $T_{c2}(H) < T < T_{c3}(H)$  and become linear only when  $T_{c3}(H)$  is exceeded. In the inset we present the derivative of the measured  $I$ - $V$  curves. We see that even at  $T=3.9$  K the response is nonlinear in small applied currents. In agreement to other works the experimental

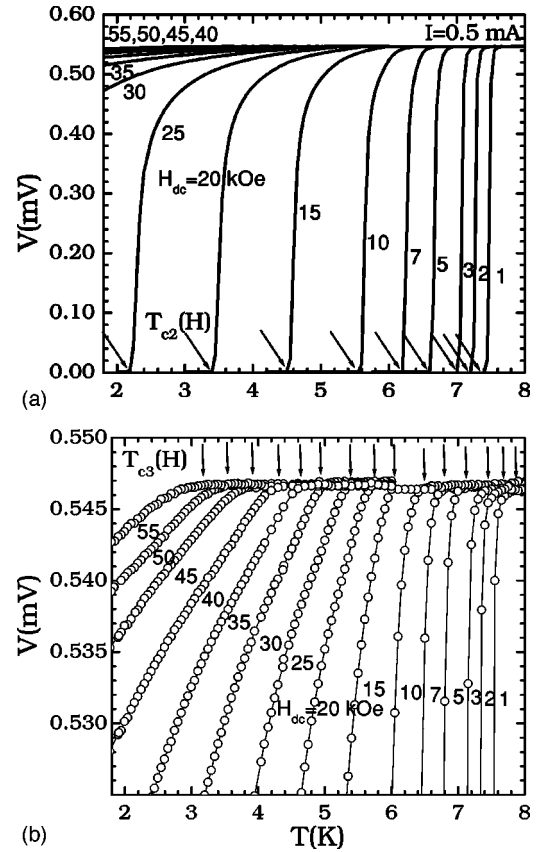


FIG. 2. Measured voltage in the HS as a function of temperature for various dc magnetic fields under a dc transport current  $I_{dc} = 0.5$  mA ( $J_{dc} \approx 80$  A/cm<sup>2</sup>) when the dc field is normal to the surface of the film. The upper panel presents the whole resistive transition, while in the lower panel we focus in the regime where the voltage attains its normal state value.

data presented in Fig. 3 give evidence that the regime  $T_{c2}(H) < T < T_{c3}(H)$  is governed by surface superconductivity.<sup>25,26,28,30-33</sup> Although the original theory predicted the presence of the effect only for the case where the field is parallel to the surface of the specimen, recent experimental reports investigated also the case where the field is normal to the surface of the sample giving evidence that an analogous effect takes place even for such configuration.<sup>28,30,31</sup>

Since the MN exhibit anisotropic magnetization, different behaviors should be observed when the magnetic field is normal or parallel to the HS film. In Fig. 4 we comparatively present such measurements for both field configurations. At the first set the field was normal (open circles) while at the second set was parallel (solid circles) to the surface of the film. In both sets the dc transport current was transverse to the magnetic field. As we clearly see the resistive transition for the case where the field is normal to the surface of the HS film is rounded and more extended compared to the one for the case where the field is parallel to the film's surface.

In Fig. 5 we present in reduced temperature units a comparison of the voltage measured in pure Nb and HS films under a magnetic field  $H_{dc}=20$  kOe normal to their surfaces. We see that the upper-critical points  $T_{c2}(20$  kOe) almost co-

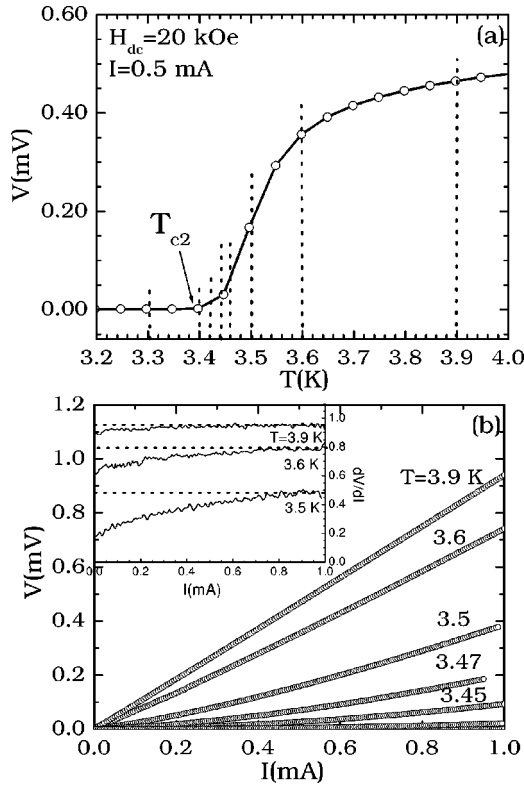


FIG. 3. Measured voltage in the HS as a function of temperature for  $I_{dc}=0.5$  mA (upper panel) and representative  $I-V$  characteristics (lower panel) at the temperatures indicated by the dotted lines. The data refer to  $H_{dc}=20$  kOe normal to the surface of the film. The inset presents the derivative of the measured  $I-V$  curves for  $T=3.5, 3.6,$  and  $3.9$  K. Even at  $T=3.9$  K the  $I-V$  curve is nonlinear in low applied currents.

incide (see the inset) but the voltage attains its normal state value at a much higher temperature  $T_{c3}$  (20 kOe) for the HS film compared to the pure Nb one. On the other hand, the corresponding measurements performed for the configuration where the applied magnetic field is parallel to the main surface of the films exhibited a totally different behavior. In the parallel configuration the  $T_{c3}$  (20 kOe) points of the HS and of the pure Nb films coincide when plotted in reduced temperature units [see the inset of Fig. 6 below].

The experimental results presented above are summarized in Figs. 6(a) and 6(b). Figure 6(a) presents the surface superconductivity fields  $H_{c3}(T)$  for the HS film for the case where the field is normal (open and solid circles) and parallel (semifilled circles) to the surface of the film. The open (solid) circles come from isofield (isothermal) measurements as a function of temperature (field). We see that for the two field configurations the characteristic lines  $H_{c3}(T)$  clearly coincide up to a certain magnetic field  $H \approx 10$  kOe, but above this value the two lines strongly diverge. Figure 6(b) summarizes the main result of the present study referring to the configuration where the field is normal to the film's surface. The  $H_{c2}(T)$  and the  $H_{c3}(T)$  lines of the HS and of the pure Nb films are presented in reduced temperature units. The  $H_{c2}(T)$  lines are determined by magnetic (open and solid rhombi for the HS film) and magnetoresistance measure-

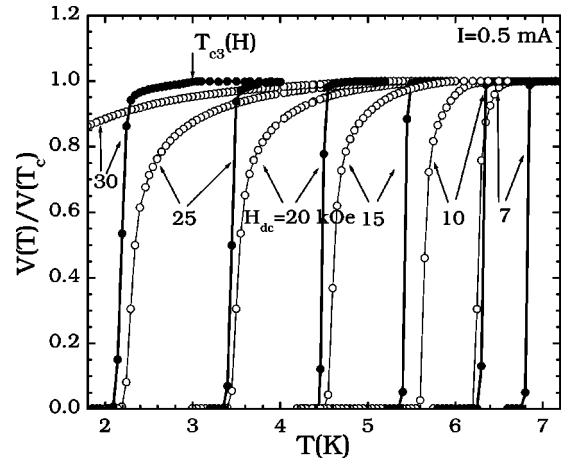


FIG. 4. Measured voltage on the HS film as a function of temperature for various dc magnetic fields under a dc transport current  $I_{dc}=0.5$  mA ( $J_{dc} \approx 80$  A/cm<sup>2</sup>) when the dc field is normal (open circles) and when it is parallel (solid circles) to the surface of the film. In both cases the transport current is transverse to the magnetic field.

ments (triangles and semifilled rhombi for the pure Nb and HS films, respectively). The most important result presented in Fig. 6(b) is that the characteristic lines  $H_{c3}(T)$  coincide up to  $H \approx 10$  kOe but above this field they strongly segregate, with the  $H_{c3}(T)$  line of the HS film placed at much higher fields comparing to the respective one of pure Nb. The characteristic value  $H \approx 10$  kOe is equal to the saturation field of the MN. This experimental fact gives strong evidence that the MN are responsible for the behavior observed in  $H_{c3}(T)$  (see below). Furthermore, above  $H \approx 10$  kOe the bulk uppercritical field line  $H_{c2}(T)$  of the HS presents a smooth deviation from the extrapolated high temperature data (see dotted line). This behavior is not observed in the  $H_{c2}(T)$  data of pure Nb. Thus, regarding  $H_{c2}(T)$  the preliminary results presented in this work suggest that the weak rounding observed

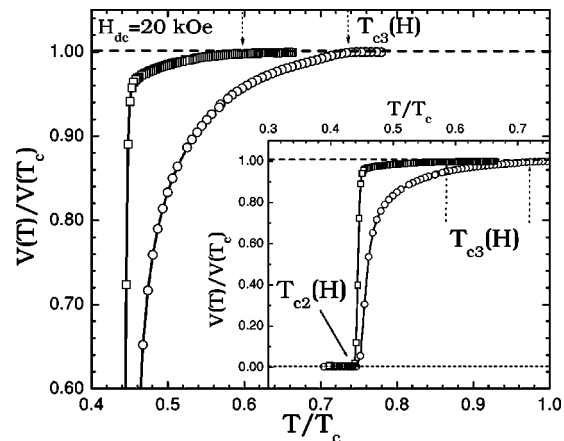


FIG. 5. Comparison of the measured normalized voltage for the pure Nb (squares) and the HS (circles) films as a function of reduced temperature under a dc transport current  $I_{dc}=0.5$  mA ( $J_{dc} \approx 80$  A/cm<sup>2</sup>) for  $H_{dc}=20$  kOe. In both measurements the magnetic field is normal to the surface of the film.

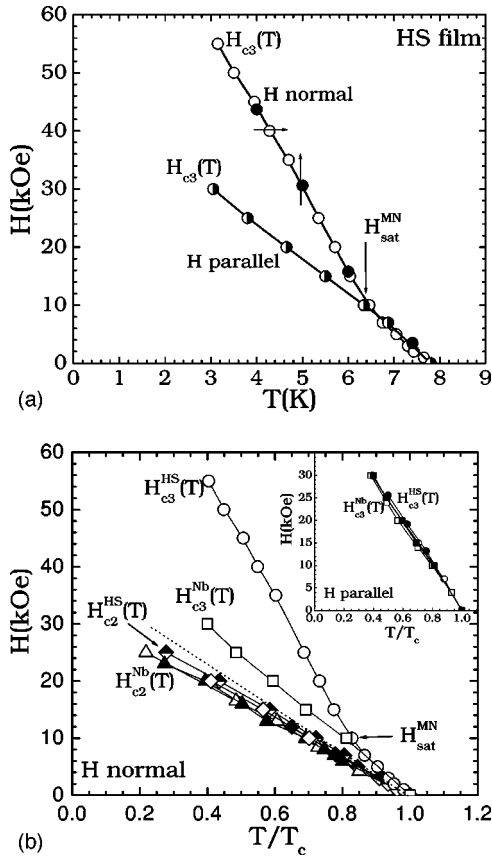


FIG. 6. The upper panel presents the characteristic field lines  $H_{c3}(T)$  where the voltage attains its normal state value for the HS film measured when the magnetic field is normal (open and solid circles) and when it is parallel (semifilled circles) to the surface of the film. In the lower panel and in reduced temperature presented are the upper-critical field lines  $H_{c2}(T)$  (triangles and rhombi for the Nb and the HS films, respectively), and the characteristic fields  $H_{c3}(T)$  where the voltage attains its normal state value, of the pure Nb (squares) and HS (circles) films measured when the magnetic field is normal to the surface of the film. In the inset we present the  $H_{c3}(T)$  lines for the pure Nb (squares) and for the HS (circles) films measured when the magnetic field is parallel to the surface of the film. In all cases the transport current is transverse to the magnetic field.

in the line  $H_{c2}(T)$  of the HS is motivated by the MN [as is the pronounced one observed in the line  $H_{c3}(T)$ ]. Despite that, this gradual deviation could be also ascribed to the common zeroing of its slope as the line  $H_{c2}(T)$  of a disordered superconductor approaches zero temperature. In this work we focus on the pronounced effect observed in  $H_{c3}(T)$  and we will not refer further on the weak rounding observed in  $H_{c2}(T)$  since more experiments are needed to clarify this point. By extrapolating the related data to zero temperature we find that the ratio of the surface superconductivity field  $H_{c3}(T)$  to the bulk upper-critical field  $H_{c2}(T)$  is  $H_{c3}(0)/H_{c2}(0) = 1.5$  and 2.9 for the pure Nb and the HS films, respectively. The estimated value  $H_{c3}(0)/H_{c2}(0) = 1.5$  for the pure Nb film is close to the theoretically proposed value of 1.695.<sup>25,26</sup> In contrast, the corresponding value  $H_{c3}(0)/H_{c2}(0) = 2.9$  for the HS film is strongly increased. For the case where the magnetic field is

parallel to the surface of the films the situation is entirely different as presented in the inset in reduced temperature units. We observe that the lines  $H_{c3}(T)$  of the pure Nb (squares) and HS (circles) films almost coincide in the whole temperature-magnetic-field regime investigated in this work.

As we mentioned in the introduction there are two basic mechanisms that control the interaction between the superconducting order parameter and the magnetic moments at a SC/FM bilayer. First is the electromagnetic mechanism and second is the exchange interaction that the superconducting pairs experience as they enter the FM through the SC/FM interface. The second mechanism results in a strong depression of the superconducting order parameter at the surfaces of a SC which are placed in close proximity to the FM component (proximity effect).<sup>14–16</sup> In contrast, at a SC/IN interface the surface superconductivity effect implies that for magnetic fields  $H_{c2}(T) < H < H_{c3}(T)$  the superconducting order parameter is enhanced near the surfaces of the SC. Consequently, the so-called proximity effect should act against the formation of surface superconductivity. Our data give evidence for an enhancement of surface superconductivity in the HS film. Thus, we speculate that probably the proximity effect does not have strong influence in our case. One way to eliminate the proximity effect is by placing a sufficiently thick insulating spacer between the SC and the FM components. In such structures the insulating layer ensures that the superconducting pairs do not experience the dominant exchange interactions as they never enter the FM. On the other hand, recent studies<sup>17–22</sup> showed that an important phenomenological parameter called transparency should be introduced in order for the theory to be consistent with the experimental results. This parameter which describes the transmission ability of the SC/FM interface depends on extrinsic and intrinsic factors. The main extrinsic contribution comes from the structural quality of the SC/FM interface (compositional disorder, oxidation, mismatch of the lattices that results in strain effects),<sup>17,20–22</sup> while the intrinsic one is related to the specific spin-dependent scattering mechanism that the superconducting pairs experience as they go through the interface.<sup>17,20,34</sup> For the case of perfect SC/FM surfaces the transparency is maximum and as a result the proximity effect may be easily observed. In contrast, strongly disordered interfaces are described by low transparency and the proximity effect could be strongly depressed. Due to the preparation technique employed in our work the produced MN do not have flat surfaces, in contrast to other works where the magnetic dots or squares were usually fabricated by means of a controllable lithographic technique. Thus, in our case the proximity effect could be strongly depressed due to structural distortion and possible oxidation of the SC/FM interfaces.

In order to leave no doubt, below we compare our experimental results with recent theoretical studies<sup>35</sup> and experimental works<sup>3,36–41</sup> that refer to similar phenomena motivated by the proximity effect in superconducting-normal metal (SC/NM) or SC/FM multilayers. In recent studies Takahashi and Tachiki<sup>35</sup> suggested that due to the proximity effect a strong deviation in the bulk upper-critical field  $H_{c2}(T)$  should be observed in a SC/NM multilayer. A brief summary of their conclusions is given here. The constituent

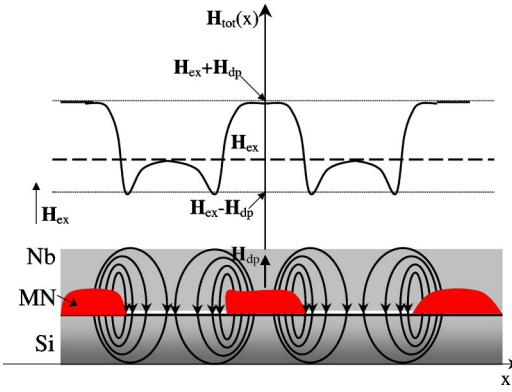


FIG. 7. Schematic presentation of the HS consisting of the MN embedded at the bottom of the Nb layer. The external applied field  $\mathbf{H}_{\text{ex}}$  (thick dashed line) is modulated by the dipolar fields  $\mathbf{H}_{\text{dp}}$  of the MN. Due to the inhomogeneous intensity of the dipolar fields, the total local field  $\mathbf{H}_{\text{tot}}$  (thick solid curve) presents a local minimum very close to the lateral surfaces of the MN. Away from the MN the total local field equals the external field.

layers of the superlattice are characterized by their diffusion constants  $D$ , pairing potentials  $V$ , electronic density of states  $\Lambda$  and thicknesses  $d$ . By varying each parameter separately the authors<sup>35</sup> showed that both parallel and normal bulk upper-critical fields exhibit an intense change at some characteristic temperature. First, let us suppose that only  $\Lambda$  is discontinuous at the SC/NM interface, while  $D_S = D_N$ ,  $V_S = V_N$ , and  $d_S = d_N$ . For temperatures close to  $T_c$  the usual three-dimensional linear behavior is observed in the parallel bulk upper-critical field  $H_{\parallel c2}(T) \propto (1 - T/T_0)$ . When decreasing the temperature the superconducting coherence length  $\xi_S$  also decreases and at a characteristic temperature it becomes equal both to  $d_S$  and  $d_N$ . Below this characteristic temperature,  $H_{\parallel c2}(T)$  exhibits a square-root dependence  $H_{\parallel c2}(T) \propto (1 - T/T_0)^{1/2}$  which is indicative of a two-dimensional behavior. Thus, in the low temperature regime the layers of the SC become decoupled. The same qualitative behavior is also observed in  $H_{\parallel c2}(T)$  when the conditions  $\Lambda_S = \Lambda_N$ ,  $V_S = V_N$  and  $d_S = d_N$  hold, but the diffusion constants of the constituent layers are unequal,  $D_S \neq D_N$ . In the later case the effect is even more dramatic for the normal upper-critical field  $H_{\perp c2}(T)$ . While close to the critical temperature the  $H_{\perp c2}(T)$  exhibits the usual linear behavior, below a characteristic temperature acquires a pronounced upturn. It is worth noting that in contrast to  $H_{\parallel c2}(T)$  the  $H_{\perp c2}(T)$  exhibits almost linear behavior in a wide regime both below and above the characteristic temperature. This is reminiscent of the behavior observed in our data. Thus, a comparison of the two cases is necessary. Due to the fact that the CoPt MN are embedded at the bottom of the Nb film a normal applied magnetic field could be experienced as parallel by the sequential (but not periodic) lateral MN/Nb interfaces (see Fig. 7 below). So, the present experimental configuration could be analogous, in some degree, to the theoretically described<sup>35</sup> and experimentally studied artificial SC/NM<sup>36-40</sup> or SC/FM<sup>3,41</sup> multilayers. Interestingly, the shape of the resulting line  $H_{c3}(T)$  observed in our case is similar to the one exhibited by the *parallel* “upper-critical field”  $H_{\parallel c2}(T)$  when a crossover from three-

dimensional to two-dimensional behavior was observed in the above-mentioned experimental and theoretical reports.<sup>35-37,41</sup> Despite this similarity there are also strong differences that should be mentioned. First of all, we have to underline that in those works absolutely *periodic* multilayered structures were employed, while in our case we have a nonperiodic distribution in the MN/Nb interfaces. Second, our  $H_{c3}(T)$  data do not exhibit a  $(1 - T/T_0)^{1/2}$  dependence in the low temperature regime. Third and more important, our experimental data refer to the surface superconductivity field line  $H_{c3}(T)$  and not to the bulk upper-critical fields  $H_{c2}(T)$ . Due to the above arguments we believe that either the behavior observed in our  $H_{c3}(T)$  data is not influenced by the proximity effect, or the results of previously published experimental works refer also to the surface superconductivity field  $H_{c3}(T)$ . The second case is possible since in most works the upper-critical field was usually defined by the midpoints of the resistive transition without comparing with magnetic measurements. As a consequence, the data presented in the past could more or less detect  $H_{c3}(T)$  and not  $H_{c2}(T)$ . Finally, we note that until today there is no theoretical work investigating the problem of a thick SC layer in proximity with a FM in the field range  $H_{c2}(T) < H < H_{c3}(T)$  where surface superconductivity is expected in the SC. The antagonistic role of the proximity effect and surface superconductivity strongly complicates this problem. Our experimental results could give some information for future theoretical treatment of this problem.

By assuming that in our case the electromagnetic mechanism dominates over the proximity effect, in the discussion given below we propose a simple explanation for our experimental results. Magnetization loop measurements performed in the HS film in temperature just above  $T_c$  (not shown here) revealed that the saturation field of the MN is  $H_{\text{sat}}^{\text{MN}} \approx 10$  kOe (see also Ref. 29). This value is equal to the characteristic field above (below) which the respective lines  $H_{c3}(T)$  of the HS and the pure Nb films diverge (coincide) when the field is normal to the film’s surface. We believe that this *purely experimental fact* may lead us to the following qualitative interpretation for the behavior observed in Figs. 6(a) and 6(b). Under zero magnetic field the anisotropic MN have their moments randomly distributed so their macroscopic magnetic moment is zero. When we apply the magnetic field normal to the film we also align the dipolar fields of the MN normal to the film’s surface. The situation discussed here is schematically presented in Fig. 7. The dipolar fields  $\mathbf{H}_{\text{dp}}$  will reduce (enhance) the external applied field  $\mathbf{H}_{\text{ex}}$  in the region by the lateral surfaces of the MN (in the region above their normal surfaces), so that the total effective magnetic field  $\mathbf{H}_{\text{tot}}$  is lower (higher) than the external magnetic field in the respective regimes. As our experimental results showed, the whole effect takes place clearly above the bulk upper-critical-field line  $H_{c2}(T)$ , so that the dipolar fields  $\mathbf{H}_{\text{dp}}$  of the MN are not efficient to reduce the external applied field  $\mathbf{H}_{\text{ex}}$  in the bulk of the superconductor and drive it in the mixed state. More importantly, we believe that the observed effect is related to the fine local *uneven* distribution in the intensities of the dipolar fields  $\mathbf{H}_{\text{dp}}$  (see Fig. 7). The dipolar fields of the MN are not uniform in the surrounding space

but have higher intensity in the vicinity close to their lateral surfaces, while away from them decay rapidly to zero. This could lead to a more efficient compensation of the external magnetic field in the vicinity by the lateral surfaces of the MN. Such a reduction of the external field could enhance the formation of a superconducting condensate confined close to the lateral surfaces of the MN, thus promoting surface superconductivity.

Finally, we discuss another possible mechanism that could motivate the rounding observed in our resistance curves. Due to their preparation procedure the MN are not identical but a distribution in their sizes exist. Although the distribution of their in-plane dimensions could possibly assist a rounding in the measured voltage curves, it could not be the main underlying mechanism that motivates the observed effect. A distribution in their out-of-plane dimension (height) also exists and this should also lead to the same effect when the field is parallel to the film's surface. This is not observed in our results. Consequently, we believe that the distribution in the dimensions of the MN could not be the main reason for the observed effect.

#### IV. CONCLUSIONS

In conclusion, we presented detailed transport and magnetic measurements in pure Nb and in HS films in the whole temperature-magnetic-field regime accessible by our SQUID. We observed that when the magnetic field is parallel to their surfaces the characteristic lines  $H_{c3}(T)$  coincide en-

tirely when plotted in reduced temperature units. In contrast, the situation changes strongly when the field is normal to the surface of the films. Although for this field configuration the bulk upper-critical fields  $H_{c2}(T)$  of the two films almost coincide in the entire temperature regime, their respective characteristic lines  $H_{c3}(T)$  coincide up to the saturation field  $H_{\text{sat}}^{\text{MN}} \approx 10$  kOe of the MN, while above this field they strongly segregate. In our case the proximity effect is possibly depressed due to the strongly distorted surfaces of the MN. More importantly, recent works suggest that the proximity effect has a strong influence on the bulk upper-critical fields  $H_{c2}(T)$ , while our experimental results refer to the surface superconductivity field  $H_{c3}(T)$ . Thus we believe that in our case the electromagnetic mechanism is dominant and motivates the observed behavior. Consequently, we propose that in our HS film the enhancement of surface superconductivity could be ascribed to the reduction of the external applied field by the uneven dipolar fields of the MN in the vicinity by their lateral surfaces. We hope that our experimental results will promote future theoretical studies on the possible coexistence of surface superconductivity and exchange interactions at a bilayer of a thick SC placed in proximity with a FM.

#### ACKNOWLEDGMENT

This work was supported by the IHP Network "Quantum Magnetic Dots" Contract No. HPRN-CT-2000-00134 EU.

- 
- <sup>1</sup>M. Lange, M. J. Van Bael, Y. Bruynseraede, and V. V. Moshchalkov, Phys. Rev. Lett. **90**, 197006 (2003).  
<sup>2</sup>L. E. Helseth, P. E. Goa, H. Hauglin, M. Baziljevich, and T. H. Johansen, Phys. Rev. B **65**, 132514 (2002).  
<sup>3</sup>H. Homma, C. S. L. Chun, G. G. Zheng, and I. K. Schuller, Phys. Rev. B **33**, R3562 (1986).  
<sup>4</sup>F. S. Bergeret, A. F. Volkov, and K. B. Efetov, Phys. Rev. B **68**, 064513 (2003).  
<sup>5</sup>M. Baert, V. Metlushko, R. Jonckheere, V. V. Moshchalkov, and Y. Bruynseraede, Phys. Rev. Lett. **74**, 3269 (1995).  
<sup>6</sup>J. I. Martin, M. Velez, A. Hoffmann, I. K. Schuller, and J. L. Vicent, Phys. Rev. Lett. **83**, 1022 (1999).  
<sup>7</sup>D. J. Morgan, and J. B. Ketterson, Phys. Rev. Lett. **80**, 3614 (1998).  
<sup>8</sup>V. Metlushko, U. Welp, G. W. Crabtree, R. Osgood, S. D. Bader, L. E. DeLong, Z. Zhang, S. R. J. Brueck, B. Ilic, K. Chung, and P. Hesketh, Phys. Rev. B **60**, R12 585 (1999).  
<sup>9</sup>J. I. Martin, M. Velez, A. Hoffmann, I. K. Schuller, and J. L. Vicent, Phys. Rev. B **62**, 9110 (2000).  
<sup>10</sup>M. J. Van Bael, K. Temst, V. V. Moshchalkov, and Y. Bruynseraede, Phys. Rev. B **59**, 14 674 (1999).  
<sup>11</sup>O. M. Stoll, M. I. Montero, J. Guimpel, J. J. Akerman, and I. K. Schuller, Phys. Rev. B **65**, 104518 (2002).  
<sup>12</sup>A. Terentiev, B. Watkins, L. E. De Long, L. D. Cooley, D. J. Morgan, and J. B. Ketterson, Physica C **332**, 5 (2000).  
<sup>13</sup>J. I. Martin, M. Velez, E. M. Gonzalez, A. Hoffmann, D. Jaque, M. I. Montero, E. Navarro, J. E. Villegas, Ivan K. Schuller, and J. L. Vicent, Physica C **369**, 135 (2002).  
<sup>14</sup>A. Yu. Aladyshkin, A. I. Buzdin, A. A. Fraerman, A. S. Mel'nikov, D. A. Ryzhov, and A. V. Sokolov, Phys. Rev. B **68**, 184508 (2003).  
<sup>15</sup>A. I. Buzdin and A. S. Mel'nikov, Phys. Rev. B **67**, 020503(R) (2003).  
<sup>16</sup>V. L. Ginzburg, Zh. Eksp. Teor. Fiz. **31**, 202 (1956) [Sov. Phys. JETP **4**, 153 (1956)].  
<sup>17</sup>J. Aarts, J. M. E. Geers, E. Brück, A. A. Golubov, and R. Coehoorn, Phys. Rev. B **56**, 2779 (1997).  
<sup>18</sup>J. M. E. Geers, M. B. S. Hesselberth, J. Aarts, and A. A. Golubov, Phys. Rev. B **64**, 094506 (2001).  
<sup>19</sup>M. G. Khusainov and Yu. N. Proshin, Phys. Rev. B **56**, R14 283 (1997).  
<sup>20</sup>L. Lazar, K. Westerholt, H. Zabel, L. R. Tagirov, Yu. V. Goryunov, N. N. Garif'yanov, and I. A. Garifullin, Phys. Rev. B **61**, 3711 (2000).  
<sup>21</sup>I. Baladié and A. Buzdin, Phys. Rev. B **64**, 224514 (2001).  
<sup>22</sup>C. Cirillo, S. L. Prischepa, M. Salvato, and C. Attanasio, Eur. Phys. J. B **38**, 59 (2004).  
<sup>23</sup>P. G. de Gennes and G. Sarma, J. Appl. Phys. **34**, 1380 (1963).  
<sup>24</sup>E. A. Demler, G. B. Arnold, and M. R. Beasley, Phys. Rev. B **55**, 15 174 (1997), and references therein.  
<sup>25</sup>D. Saint-James, and P. G. Gennes, Phys. Lett. **7**, 306 (1963).  
<sup>26</sup>A. A. Abrikosov, *Fundamentals of the Theory of Metals* (North-

- Holland, Amsterdam, 1988).
- <sup>27</sup>Sa-Lin Cheng, and H. A. Fertig, Phys. Rev. B **60**, 13 107 (1999).
- <sup>28</sup>D. Stamopoulos, A. Speliotis, and D. Niarchos, Supercond. Sci. Technol. (to be published).
- <sup>29</sup>V. Karanasos, I. Panagiotopoulos, D. Niarchos, H. Okumura, and G. C. Hadjipanayis, Appl. Phys. Lett. **79**, 1255 (2001).
- <sup>30</sup>U. Welp *et al.*, Physica C **385**, 154 (2003); Phys. Rev. B **67**, 012505 (2003).
- <sup>31</sup>A. Rydh, U. Welp, J. M. Hiller, A. E. Koshelev, W. K. Kwok, G. W. Crabtree, K. H. P. Kim, K. H. Kim, C. U. Jung, H.-S. Lee, B. Kang, and S.-I. Lee, Phys. Rev. B **68**, 172502 (2003).
- <sup>32</sup>C. F. Hempstead and Y. B. Kim, Phys. Rev. Lett. **12**, 145 (1964).
- <sup>33</sup>W. DeSorbo, Phys. Rev. **135**, A1190 (1964).
- <sup>34</sup>M. J. M. de Jong, and C. W. J. Beenakker, Phys. Rev. Lett. **74**, 1657 (1995).
- <sup>35</sup>S. Takahashi, and M. Tachiki, Phys. Rev. B **33**, 4620 (1986); **34**, 3162 (1986); **35**, 145 (1987).
- <sup>36</sup>K. Kanoda, H. Mazaki, T. Yamada, N. Hosoi, and T. Shinjo, Phys. Rev. B **33**, 2052 (1986).
- <sup>37</sup>I. Banerjee, Q. S. Yang, C. M. Falco, and I. K. Schuller, Phys. Rev. B **28**, 5037 (1983).
- <sup>38</sup>C. S. L. Chun, G.-G. Zheng, J. L. Vicent, and I. K. Schuller, Phys. Rev. B **29**, 4915 (1984).
- <sup>39</sup>A. Sidorenko, C. Surgers, T. Trappmann, and H. v. Lhneysen, Phys. Rev. B **53**, 11 751 (1996).
- <sup>40</sup>J. D. Hettinger, B. R. Washburn, N. B. Remmes, D. G. Steel, K. E. Gray, E. E. Fullerton, and C. H. Sowers, Phys. Rev. Lett. **77**, 5280 (1996).
- <sup>41</sup>J. S. Jiang, D. Davidovic, D. H. Reich, and C. L. Chien, Phys. Rev. B **54**, 6119 (1996).